Acta Cryst. (1967). **22**, 615

Fourier Transform Methods for Random-Layer Line Profiles

BY W. RULAND

Union Carbide European Research Associates, S.A., 95 rue Gatti de Gamond, Brussels 18, Belgium

(*Received* 6 *July* 1966)

The problem of the synthesis and the analysis of random-layer line profiles arises in the evaluation of X-ray diagrams of disordered lamellar structures, for example non-graphitic carbons. It is shown that the exact solution of the problem (evaluating the spherical average of a rod-like intensity distribution) and the circular cylinder approximation can be given in a closed form involving Fourier sine transforms and Fourier Bessel transforms respectively. For intensity distributions of the Cauchy type, analytical expressions for the exact solution, for the circular cylinder approximation, and for the approximations given by Warren and by Wilson are found, which facilitate the evaluation of the range of validity of the approximations. Based on the information obtained from this comparison a method for the analysis of random-layer line profiles is developed which uses a general Fourier transformation with subsequent refinement to compute the Fourier transform of the cross section of the rod-like intensity distribution and thus permits the investigation of line profiles from random-layer structures in the same way as line profiles form three-dimensional lattices.

Introduction

The intensity diffracted by a two-dimensional lattice is represented in reciprocal space by a periodic array of parallel rod-like intensity distributions. A random distribution of two-dimensional lattices poses the problem of taking the spherical average over such a distribution. This problem was first treated by von Laue (1932) for an infinitely thin rod by approximating the averaging sphere by tangent planes. The resulting intensity distribution is given by

$$I(s)=\frac{1}{2\pi s\sqrt{(s^2-s_h^2)}} \quad \text{for } s>s_h$$
$$I(s)=0 \quad \text{for } s<s_h \qquad (1)$$

where $I(s)$ is the intensity as a function of the absolute value of the reciprocal space vector ($s=2\sin\theta/\lambda$) and s_h the distance of the rod of index $\mathbf{h}$ ($=hk$) from the origin of reciprocal space. The intensity along the rod is considered to be unity.

For a rod of finite diameter, Warren (1941) has developed an approximation which is given by

$$I(s)=\frac{1}{\pi s\sqrt{(2s)}}\int_0^\infty \{I_h\}(s-s_h-z^2)dz \qquad (2)$$

when normalized as equation (1). $\{I_h\}(s)$ is the normalized projection of the cross section of the rod on to the plane defined by the origin of reciprocal space and the axis of the rod. Warren (1941) has evaluated the integral for I_h in the form of a Gaussian distribution and has shown that the validity of (2) is restricted to values of s in the vicinity of s_h.

Recently, Warren & Bodenstein (1966) have modified this approximation to

$$I(s)=\frac{1}{\pi s\sqrt{(s+s_h)}}\int_0^\infty \{I_h\}(s-s_h-z^2)dz\,, \qquad (3)$$

which also holds for $s_h \gg s$, and have evaluated the integral taking the exact expression of I_h for circular disks.

Wilson (1949) has given a more general treatment of the problem including the possibility of intensity variations along the rod. If the latter can be neglected he derived an expression for the line profile given by

$$I(s)=\frac{1}{2\pi s\sqrt{(2s_h)}}\int_0^\infty \frac{A_h(r)}{\sqrt{r}}(\cos 2\pi\sigma r+\sin 2\pi\sigma r)dr \qquad (4)$$

when normalized as equation (1), where A_h is the Fourier transform of $\{I_h\}$ (which is considered to be real and even) and $\sigma=(s^2-s_h^2)/2s_h$.

Brindley & Méring (1951) have considered the possibilities of taking the average numerically, using $\{I_h\}$ curves for various layer shapes.

The work presented in this paper deals with the applicability of Fourier transform methods for the synthesis and analysis of random-layer line profiles.

Exact solution

Let $I(\mathbf{s})$ be the intensity distribution in reciprocal space ($s=2\sin\theta/\lambda$) for a pair of rods of opposite index, the axes of which are located at $\mathbf{s}=\mathbf{s}_h$ and $\mathbf{s}=-\mathbf{s}_h$. If the intensity distribution in the cross section of a rod is $I_h(\mathbf{s}_{12})$, $\mathbf{s}_{12}$ being a vector normal to the rod axis, the normalized intensity distribution is given by

$$I(\mathbf{s})=\tfrac{1}{2}[I_h(\mathbf{s}_{12}-\mathbf{s}_h)+I_h(-\mathbf{s}_{12}+\mathbf{s}_h)]\,. \qquad (5)$$

The Fourier tansform of $I(\mathbf{s})$ is

$$P(\mathbf{r})=\int_v I(\mathbf{s})\exp(2\pi i\mathbf{rs})dv_s$$
$$=\delta(\mathbf{r}_3)[A_h(\mathbf{r}_{12})\cos 2\pi\mathbf{s}_h\mathbf{r}_{12}-B_h(\mathbf{r}_{12})\sin 2\pi\mathbf{s}_h\mathbf{r}_{12}]$$

where A_h and B_h are the real and the imaginary parts, respectively, of the Fourier transform of I_h, δ is the Dirac delta distribution, $\mathbf{r}_{12}$ is a vector in a plane in

Fourier space which corresponds to the plane of the vectors $\mathbf{s}_{12}$, and $\mathbf{r}_3$ is a vector perpendicular to this plane.

The spherical average of $P(\mathbf{r})$ is given by

$$P_\omega(r) = \frac{1}{4\pi}\int_0^{\pi}\int_0^{2\pi} P(\mathbf{r}) \sin\varphi d\varphi d\psi$$

where φ and ψ are the angles of the spherical coordinates of $\mathbf{r}$. If one takes φ as the angle between $\mathbf{r}_3$ and $\mathbf{r}$ and ψ as the angle between $\mathbf{s}_h$ and $\mathbf{r}_{12}$, one finds

$$P_\omega(r) = \frac{1}{2\pi r}\int_0^{\pi}[A_h(\mathbf{r}_{12}) \cos(2\pi s_h r_{12}\cos\psi) - B_h(\mathbf{r}_{12}) \sin(2\pi s_h r_{12}\cos\psi)]d\psi\,, \quad (6)$$

from which the spherical average of $I(\mathbf{s})$ is obtained by

$$I_\omega(s) = \frac{2}{s}\int_0^{\infty} rP_\omega(r) \sin 2\pi rsdr\,. \quad (7)$$

A particularly simple form is obtained when I_h is radially symmetrical. In this case A_h is a function of the absolute value of $\mathbf{r}_{12}$ only, B_h is zero and equation (6) thus becomes

$$P_\omega(r) = \frac{1}{2r} A_h(r) J_0(2\pi s_h r) \quad (8)$$

where J_0 is the Bessel function of the first kind of zero order. Consequently, equation (7) gives

$$I_\omega(s) = \frac{1}{s}\int_0^{\infty} A_h(r) J_0(2\pi s_h r) \sin 2\pi rsdr\,. \quad (9)$$

Fig. 1 shows line profiles computed according to equation (9) with

$$A_h(r) = \frac{2}{\pi}\left[\arccos\frac{r}{2R} - \frac{r}{2R}\sqrt{\left\{1-\left(\frac{r}{2R}\right)^2\right\}}\right]$$

corresponding to the shape function of circular disks with radius R.

Tangent cylinder approximation

The spherical average of $I(\mathbf{s})$ can be approximated by a cylindrical average when the breadth of the intensity distribution in the cross section of the rod perpendicular to $\mathbf{s}_h$ is small compared with s_h. Let $\mathbf{s}$ be given by

$$\mathbf{s} = \mathbf{s}_1 + \mathbf{s}_2 + \mathbf{s}_3$$

where $\mathbf{s}_1$, $\mathbf{s}_2$ and $\mathbf{s}_3$ are mutually perpendicular and let $\mathbf{s}_1$ be in the direction of $\mathbf{s}_h$, $\mathbf{s}_3$ parallel to the axis of the rod. The spherical average of $I(\mathbf{s})$ is given by

$$I_\omega(s) = \frac{1}{4\pi}\int_0^{2\pi}\int_0^{\pi} I(\mathbf{s}) \sin\varphi d\varphi d\psi\,. \quad (10)$$

Let ψ be the angle between $\mathbf{s}_1$ and $\mathbf{s}_{12}$, the projection of $\mathbf{s}$ onto the plane defined by $\mathbf{s}_1$ and $\mathbf{s}_2$, and φ the angle between $\mathbf{s}_3$ and $\mathbf{s}$. If the breadth of the distribution $I(\mathbf{s})$ in the $\mathbf{s}_2$ direction is small, equation (10) is approximately

$$I_\omega(s) \simeq \frac{1}{2\pi}\int_{-\infty}^{\infty}\int_0^{\pi} I(\mathbf{s}) \sin\varphi d\varphi \frac{ds_2}{s_1}$$

since ψ can be approximated by s_1/s_2 and a factor 2 appears since the integration has to be carried out on both sides of the s_1 axis. Interchanging the order of integration and taking into account that s_1 is approximately $s/\sin\varphi$ for small values of s_2, one finds

$$I_\omega(s) \simeq \frac{1}{4\pi s}\int_0^{2\pi}\{I\}_2(\mathbf{s}_{13})d\varphi\,,$$

where $\{I\}_2$ is the two-dimensional projection of $I(\mathbf{s})$ onto the plane defined by $\mathbf{s}_1$ and $\mathbf{s}_3$ which, following equation (5), is given by

$$\{I\}_2(\mathbf{s}_{13}) = \tfrac{1}{2}[\{I_h\}_1(s_1 - s_h) + \{I_h\}_1(-s_1 + s_h)]\,, \quad (11)$$

where $\{I_h\}_1$ is the one-dimensional projection of $I_h(\mathbf{s}_{12})$ onto s_1.

Fourier transformation of equation (11) gives accordingly

$$P(\mathbf{r}_{13}) = \delta(r_3)\,.\,[A_h(r_1)\cos 2\pi s_h r_1 - B_h(r_1)\sin 2\pi s_h r_1]$$

and the radial average

$$\frac{1}{2\pi}\int_0^{2\pi} P(\mathbf{r}_{13})d\varphi = \frac{1}{\pi r}[A_h(r)\cos 2\pi s_h r - B_h(r)\sin 2\pi s_h r]\,.$$

By inverse transformation one finds

$$\int_0^{2\pi}\{I\}_2(\mathbf{s}_{13})d\varphi = 2\pi\int_0^{\infty} r\int_0^{2\pi} P(\mathbf{r}_{13})d\varphi J_0(2\pi sr)dr;$$

thus

$$I_\omega(s) \simeq \frac{1}{s}\int_0^{\infty}[A_h(r)\cos 2\pi s_h r - B_h(r)\sin 2\pi s_h r]J_0(2\pi sr)dr\,. \quad (12)$$

Comparison of the exact solution and the approximations

Let us assume I_h to be radially symmetrical. The exact solution as given by equation (9) can then be expressed in the form of a convolution (*) by

$$I(s) = \frac{1}{2\pi s}\left[\{I_h\}(s) * \mathrm{Re}\frac{\mathrm{sgn}(s)}{\sqrt{(s^2 - s_h^2)}}\right] \quad (13)$$

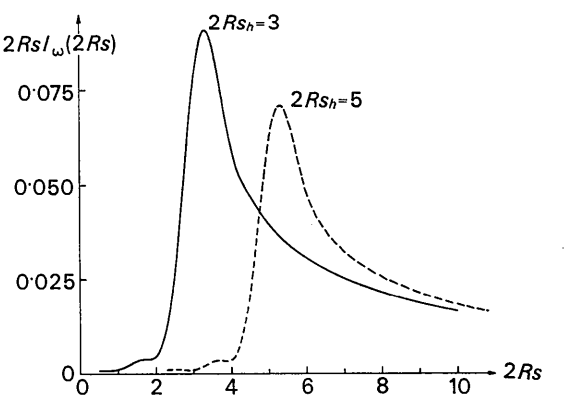

Fig. 1. Line profiles computed after equation (9) for circular disks of radius R.

since

$$\int_0^\infty A_h(r) J_0(2\pi s_h r) \sin 2\pi r s dr$$

can be written

$$\tfrac{1}{2}\int_{-\infty}^{\infty} A_h(r)\mathrm{sgn}(r) J_0(2\pi s_h r) \sin 2\pi r s dr$$

which yields

$$\left[\int_{-\infty}^{\infty} A_h(r) \cos 2\pi r s dr\right] * \left[\tfrac{1}{2}\int_{-\infty}^{\infty} \mathrm{sgn}(r) J_0(2\pi s_h r) \sin 2\pi r s dr\right] = \{I_h\}(s) * \mathrm{Re}\frac{\mathrm{sgn}(s)}{\sqrt{(s^2 - s_h^2)}},$$

where Re stands for real part and $\mathrm{sgn}(x)$ is the sign function of x.

In a similar way one derives from equation (12)

$$I(s) = \frac{1}{2\pi s}\left[I_h(s) *_2 \mathrm{Re}\frac{1}{\sqrt{(s^2 - s_h^2)}}\right], \qquad (14)$$

in which $I_h(s)$ and $\mathrm{Re}(s^2 - s_h^2)^{-\frac{1}{2}}$ have to be considered as two-dimensional distributions of radial symmetry; the convolution is thus, in contrast to equation (13), a two-dimensional one ($*_2$).

To express Wilson's equation (4) in the form of a convolution, one writes

$$\int_0^\infty \frac{1}{\sqrt{r}} A_h(r)(\cos 2\pi\sigma r + \sin 2\pi\sigma r) dr$$

$$= \tfrac{1}{2}\int_{-\infty}^{\infty} \frac{1}{\sqrt{|r|}} A_h(r)[1 - i\,\mathrm{sgn}(r)] \exp(2\pi i\sigma r) dr$$

$$= \left[\int_{-\infty}^{\infty} A_h(r) \cos 2\pi\sigma r dr\right] * \left[\tfrac{1}{2}\int_{-\infty}^{\infty} \frac{1}{\sqrt{|r|}}[1 - i\,\mathrm{sgn}(r)] \exp(2\pi i\sigma r) dr\right],$$

which yields

$$\{I_h\}(\sigma) * \mathrm{Re}\frac{1}{\sqrt{\sigma}};$$

thus

$$I(s) = \frac{1}{2\pi s\sqrt{(2s_h)}}\left[\{I_h\}(\sigma) * \mathrm{Re}\frac{1}{\sqrt{\sigma}}\right]. \qquad (15)$$

An integral of the type

$$\int_0^\infty f(x - z^2) dz$$

which is the basis of Warren's approximation can also be expressed in the form of a convolution. Substituting $y = z^2$, this integral becomes

$$\tfrac{1}{2}\int_0^\infty \frac{1}{\sqrt{y}} f(x - y) dy = \tfrac{1}{2}\left[f(x) * \mathrm{Re}\frac{1}{\sqrt{x}}\right];$$

equations (2) and (3) are thus given by

$$I(s) = \frac{1}{2\pi s\sqrt{(2s)}}\left[\{I_h\}(s) * \mathrm{Re}\frac{1}{\sqrt{(s - s_h)}}\right] \qquad (16)$$

$$I(s) = \frac{1}{2\pi s\sqrt{(s + s_h)}}\left[\{I_h\}(s) * \mathrm{Re}\frac{1}{\sqrt{(s - s_h)}}\right]. \qquad (17)$$

For large positive values of $s - s_h$ or for narrow distributions I_h all equations except (16) tend towards equation (1). In this respect the replacement of $\sqrt{(2s)}$ in (16) by $\sqrt{(s + s_h)}$ to give (17) is a substantial improvement of Warren's approximation.

Inspection of equations (15), (16) and (17) shows that the basic mathematical operations involved are the same, namely

$$f(x) * \mathrm{Re}\frac{1}{\sqrt{x}}; \qquad (18)$$

the difference between the methods is entirely due to the variables employed.

Comparing equations (13) and (17) the basis of Warren's approximation appears to consist in taking

$$\mathrm{Re}\frac{1}{\sqrt{(s^2 - s_h^2)}} = \frac{1}{\sqrt{(s + s_h)}} \cdot \mathrm{Re}\frac{1}{\sqrt{(s - s_h)}}$$

and in considering the first factor on the right hand side as slowly varying with respect to the second.

The basis of Wilson's approximation consists, on the contrary, in changing the variable of $\{I_h\}$ to σ, which is permissible when this distribution is relatively narrow.

Under the same condition (narrow width of I_h) equation (14) can be taken as an approximation for (13).

For large negative values of $(s - s_h)$, $I(s)$ is determined by the outer part of the distribution I_h. Thus, for approximations of the type (18) and an outer part of $f(x)$ of the type x^{-n} one finds I proportional to $|x|^{-n+\frac{1}{2}}$ for large negative values of x. For broadening due to particle size, n is equal to 2, which leads to the $|\sigma|^{-3/2}$ curves predicted by Wilson (1949).

No simple general approximation can be derived for the behaviour of $I(s)$ near the maximum value. It is, however, obvious that this part is predominantly determined by the inner part of I_h.

A quantitative comparison is facilitated by the fact that analytical expressions for the exact solution and for the approximations can be found for distributions $\{I_h\}$ of the Cauchy type.

Let $\{I_h\}$ be given by

$$\{I_h\}(s) = \frac{L}{1 + \pi^2 L^2 s^2},$$

where $1/L$ is the integral width. One finds

$$A_h(r) = \exp(-2|r|/L)$$

and $B_h = 0$. The exact solution obtained from equation (9) or (13) gives

$$I(s) = \frac{1}{4s}\sqrt{\frac{L}{\pi s}}\, F\left[\frac{\pi L}{2s}\left(s^2 - s_h^2 - \frac{1}{\pi^2 L^2}\right)\right] \qquad (19)$$

where

$$F(z)=\sqrt{\frac{\sqrt{(z^2+1)}+z}{z^2+1}} \text{ (see Fig. 2).}$$

The circular cylinder approximation gives after equation (12) or (14):

$$I(s)=\frac{1}{4s}\sqrt{\frac{L}{\pi s_h}}\,F\left[\frac{\pi L}{2s_h}\left(s^2-s_h^2+\frac{1}{\pi^2L^2}\right)\right], \quad (20)$$

Wilson's approximation in the form (4) or (15) gives

$$I(s)=\frac{1}{4s}\sqrt{\frac{L}{\pi s_h}}\,F\left[\frac{\pi L}{2s_h}(s^2-s_h^2)\right], \quad (21)$$

Warren's (1941) approximation (2) gives

$$I(s)=\frac{1}{4s}\sqrt{\frac{L}{\pi s}}\,F[\pi L(s-s_h)] \quad (22)$$

and Warren & Bodenstein's (1965)

$$I(s)=\frac{1}{4s}\sqrt{\frac{2L}{\pi(s+s_h)}}\,F[\pi L(s-s_h)]\,. \quad (23)$$

The function F has a maximum at $z=1/\sqrt{3}=0{\cdot}577$ and a half-peak width $b_z=6{\cdot}777$; for large positive values it approaches $\sqrt{(2/z)}$ and for large negative values $1/\sqrt{(2|z|^3)}$. For $s_h \gg 1/L$ the peak shift in $I(s)$ thus tends towards

$$s_{\max}-s_h=\frac{1}{\pi L\sqrt{3}}=\frac{0{\cdot}184}{L} \quad (24)$$

and the half-peak width towards

$$b_s=2{\cdot}157/L\,.$$

These relations can be compared with those derived by Warren (1941) for Gaussian distributions:

$$s_{\max}-s_h=0{\cdot}32/L\,,\ b_s=1{\cdot}84/L;$$

and from Warren & Bodenstein (1965) for distributions $\{I_a\}$ due to circular disks:

$$s_{\max}-s_h=0{\cdot}30/L\,,\ b_s=1{\cdot}91/L\,.$$

In all cases, L has been defined as the integral width of $\{I_h\}$ which, in the latter relations, leads to somewhat different constants from those given by Warren & Bodenstein since, with this definition, L equals $16R/3\pi$ for circular disks of radius R. The comparison shows that the constant for the peak shift is much smaller and for the width somewhat greater for Cauchy distributions than for the other two.

Obviously, the peak shift is more sensitive to particularities of the profile of $\{I_h\}$ than the half-peak width. Assuming, to a first approximation, that the peak shift is determined only by the inner part of $\{I_h\}$ (which is considered to be a symmetrical distribution) and applying the usual series development

$$\{I_h\}=\mathfrak{F}(A_h)$$
$$=2\int_0^\infty A_h(r)dr-4\pi^2s^2\int_0^\infty r^2A_h(r)dr+\ \ldots$$
$$\simeq\frac{2\int_0^\infty A_h(r)dr}{1+\pi^2s^2L^2/k^2}$$

one obtains from equation (24)

$$s_{\max}-s_h=\frac{k}{\pi L\sqrt{3}}\,, \quad (25)$$

where

$$k^2=\frac{2\left[\int_0^\infty A_h(r)dr\right]^3}{A_h^2(0)\int_0^\infty r^2A_h(r)dr}$$

and

$$L=\frac{2\int_0^\infty A_h(r)dr}{A_h(0)}\,.$$

In Table 1 values of k and $L(s_{\max}-s_h)$ are listed for line profiles due to various layer shapes calculated from the appropriate expressions for $A_h(r)$.

Table 1. *Peak shift parameters for various layer shapes*

Layer shapes or type of distribution	k	$L(s_{\max}-s_h)$
Square, side on	$\sqrt{3}$	0·318
Square, corner on, or triangle	$\frac{2}{3}\sqrt{5}$	0·274
Circular disk	$\frac{4}{\pi}\sqrt{\frac{5}{3}}$	0·302
Hexagon, side on	$\frac{8}{9}\sqrt{\frac{10}{3}}$	0·298
Hexagon, corner on	$\frac{14}{9}\sqrt{\frac{35}{31}}$	0·304
Gaussian distribution	$\sqrt{\pi}$	0·326

A comparison of the values obtained for circular disks and for Gaussian distributions with those given by Warren shows that equation (25) represents a fairly good approximation.

Simple expressions for the relationship between half-peak width and the type of the distribution I_h have not been found. For constant L, an increase in the peak

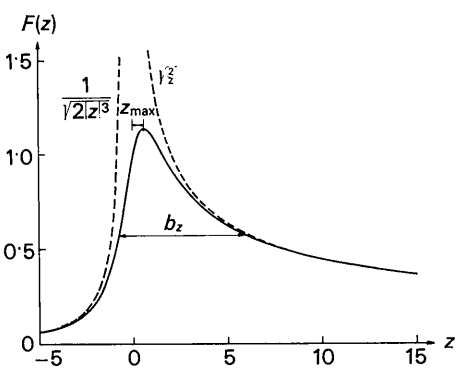

Fig. 2. The function $F(z)$ [equation (19)].

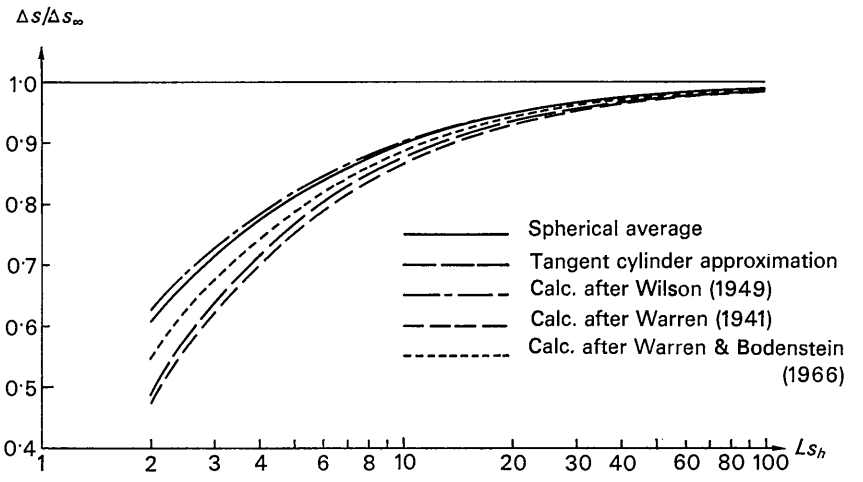

Fig. 3. Relative peak shift as function of Ls_h.

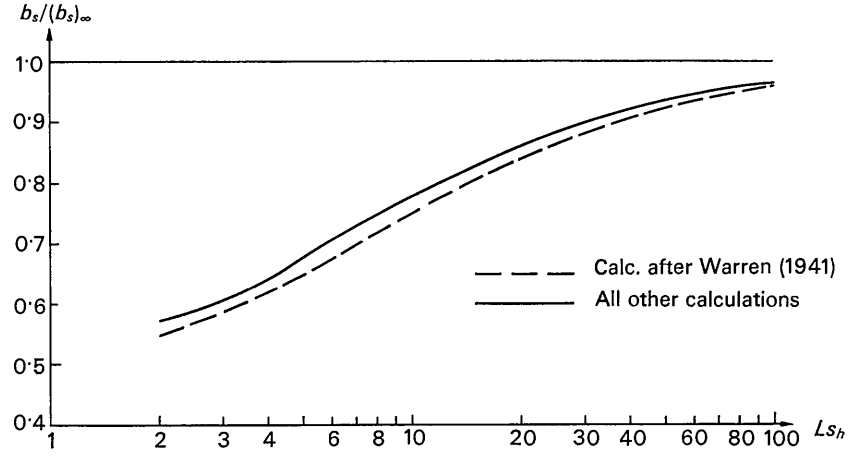

Fig. 4. Relative half-width as function of Ls_h.

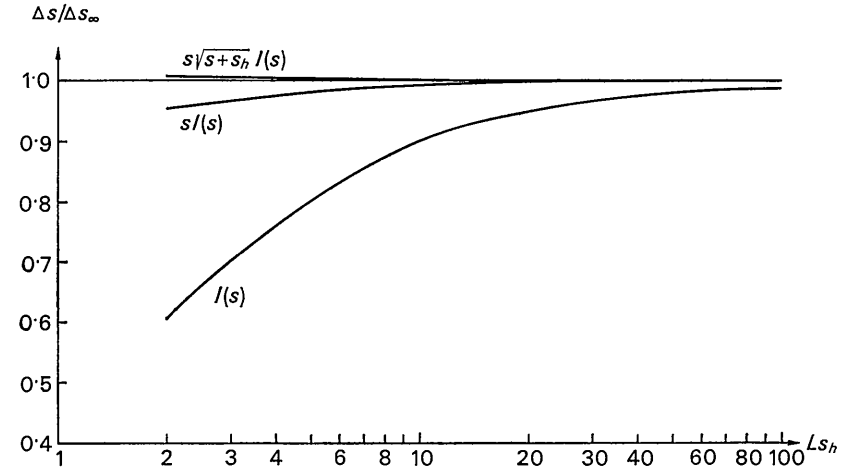

Fig. 5. Relative peak shift as function of Ls_h for $I(s)$, $sI(s)$ and $s\sqrt{(s+s_h)}\,I(s)$.

shift is obviously accompanied by a decrease in the half-peak width, the ratio of the former to the latter varying from about 0·09 for distribution of the Cauchy type to 0·18 for Gaussian distributions. For regular layer shapes and narrow size distributions the ratio will be around $0{\cdot}16 \pm 0{\cdot}02$; wide size distributions will produce lower values. The ratio of the peak shift to the half-peak width can thus be used for a qualitative characterization.

We have so far considered the characteristics of $I(s)$ for values of Ls_h large enough for the differences between the exact solution and the approximations to vanish and for angle-dependent factors to be negligible. In order to study the limitations of these conditions the peak shift and the half-peak width were evaluated from curves given by equations (19) to (23) for a series of Ls_h values ranging from 2 to 100. Figs. 3 and 4 show plots of the ratio of these parameters as functions of Ls_h to the limiting values obtained for Ls_h tending towards infinity. The results show that considerable deviations from the limiting values appear with decreasing values of Ls_h both for the peak shift and the half peak width, whereas the differences between the curves for the exact solution and those for the approximations are relatively small. In fact, the values for the half-peak width are almost identical for the exact solution and the approximations except the one given by Warren (1941). The differences are more pronounced in the case of the peak shift but are still relatively small compared with the deviations from the limiting value. It is interesting to note that the values calculated after Wilson (1949) are nearest to the exact values, followed by the values calculated after Warren & Bodenstein (1965), which are still nearer to the exact values than the values from the circular cylinder approximation. This is somewhat surprising since both methods were originally considered to be approximations of the circular cylinder.

The deviations from the limiting value can, however, be greatly reduced when the peak shift and the half-peak width are measured in $sI(s)$ curves and become negligibly small in $s\sqrt{(s+s_h)}\,I(s)$ curves as can be seen in Figs. 5 and 6, where the results obtained from plots of the exact solution are given.

Analysis of random-layer line profiles

It was shown in the preceding sections that all the expressions used to calculate random-layer line profiles can be given as Fourier transforms. Obviously, the inverse transforms should lead to the determination of A_h and B_h, the real and the imaginary part respectively of the Fourier transform of I_h, and thus permit the analysis of random-layer line profiles in the same way as line profiles from three-dimensional lattices.

The results of the last section indicate that an approximation of the type (18) appears to be fairly good for most of the Ls_h values of practical interest. Let us assume a random-layer line profile $I(s)$ to be given experimentally and suitable angle-dependent corrections already applied. From the half-peak width an approximate L value is obtained which permits the evaluation of an approximate s_h value from s_{max}.

Let us define a reduced line profile by

$$J(s') = \{I_h\}(s') * \mathrm{Re}\,\frac{1}{\sqrt{s'}} . \tag{26}$$

Leaving the normalization of I_h undefined one obtains from equation (17)

$$J(s) = s\sqrt{(s+s_h)}\,I(s)$$

and

$$s' = s - s_h .$$

For large values of s', $J(s')$ will approach the function

$$\frac{1}{\sqrt{s'}} \int_{-\infty}^{\infty} \{I_h\}(s)\,ds . \tag{27}$$

Let s_0 be the upper limit of the range of values of s in which $I(s)$ is observable. Neglecting the effect of the lower limit the reduced observable line profile is given by

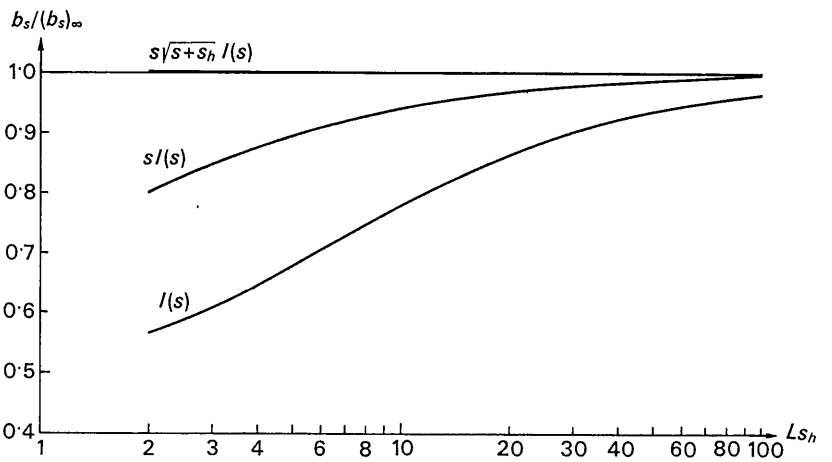

Fig. 6. Relative half-width as function of Ls_h for $I(s)$, $sI(s)$ and $s\sqrt{(s+s_h)}\,I(s)$.

$$J_{\text{obs}}(s') = \left[\{I\}(s') * \text{Re}\,\frac{1}{\sqrt{s'}}\right] . Y_{s'_0} \qquad (28)$$

where

$$s'_0 = s_0 - s_h$$

and

$$Y_{s'_0} = 1 \quad \text{for} \quad s' < s'_0$$
$$Y_{s'_0} = 0 \quad \text{for} \quad s' > s'_0 .$$

Assuming s'_0 to be in the range of values of s' where the approximation (27) is valid, equation (28) can be approximated by

$$J_{\text{obs}}(s') = \left[\{I_h\}(s') - \delta(s')\int_{-\infty}^{\infty}\{I_h\}(s)ds\right] * \text{Re}\,\frac{1}{\sqrt{s'}} + Y_{s'_0}\text{Re}\,\frac{1}{\sqrt{s'}}\int_{-\infty}^{\infty}\{I_h\}(s)ds . \qquad (29)$$

Let the Fourier transforms of $\{I_h\}$ and J_{obs} be

$$\mathfrak{F}\{I_h\} = A_h(r) + iB_h(r)$$

and

$$\mathfrak{F}(J_{\text{obs}}) = {}_0A_h(r) + i_0B_h(r) , \qquad (30)$$

respectively.

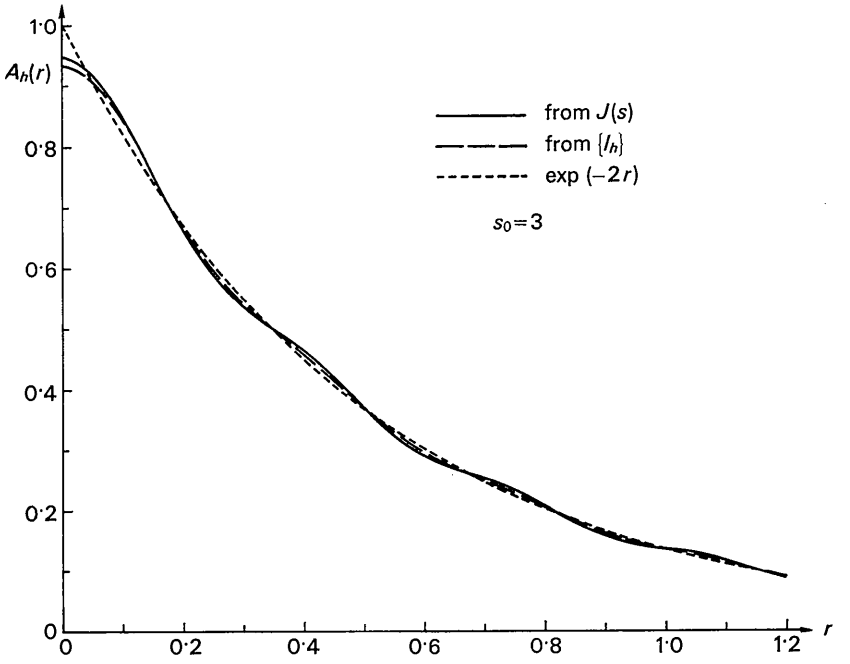

Fig. 7. Line profile analysis of $I(s)$ as given by (34).

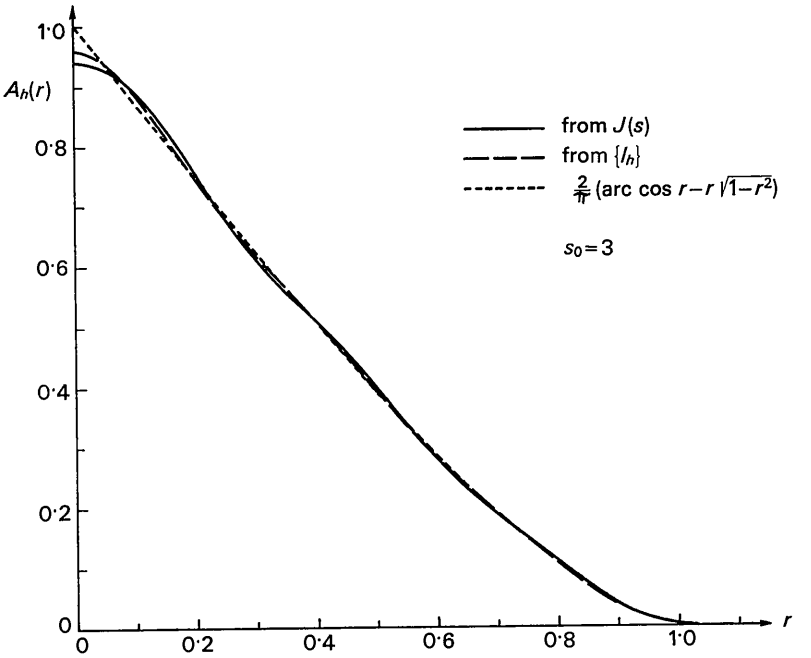

Fig. 8. Line profile analysis of $I(s)$ as given by (35).

Fourier transformation of equation (29) gives

$$\mathfrak{F}(J_{\text{obs}}) = \frac{1}{\sqrt{|r|}}\left[\tfrac{1}{2}\{A_h(r)+iB_h(r)-A_h(0)\}(1+i\,\text{sgn}(r)) + A_h(0)\{C(2\pi|r|s_0')+i\,\text{sgn}(r)S(2\pi|r|s_0')\}\right] \quad (31)$$

where $C(x)$ and $S(x)$ are the Fresnel integrals in the form

$$C(x)-iS(x)=\int_0^x \frac{e^{-it}}{\sqrt{(2\pi t)}}\,dt\,.$$

Combining equations (30) and (31) and considering that the approximation (27) implies

$${}_0A_h(0)=2\sqrt{(s_0')}A_h(0)\,,$$

one obtains the solutions

$$A_h(r)=\sqrt{r}\{{}_0A_h(r)+{}_0B_h(r)\} + \frac{{}_0A_h(0)}{2\sqrt{(s_0')}}\{1-C(2\pi rs_0')-S(2\pi rs_0')\} \quad (32)$$

and

$$B_h(r)=\sqrt{r}\{{}_0B_h(r)-{}_0A_h(r)\} + \frac{{}_0A_h(0)}{2\sqrt{(s_0')}}\{C(2\pi rs_0')-S(2\pi rs_0')\}\,. \quad (33)$$

for $r\geq 0$.

The following test functions have been chosen to check the validity of the method (s' is replaced by s for simplicity).

$$J(s)=\sqrt{(\pi/2)}F(\pi s) \quad (34)$$

corresponding to

$$\{I_h\}=\frac{1}{1+\pi^2s^2}\,,$$

$$A_h=\exp(-2|r|),\ B_h=0$$

[for $F(z)$ see equation (19)].

$J(s)$ calculated from $I_\omega(s)$ as given by equation (9) for $s_h=3$ and for circular disks of diameter unity, corresponding to

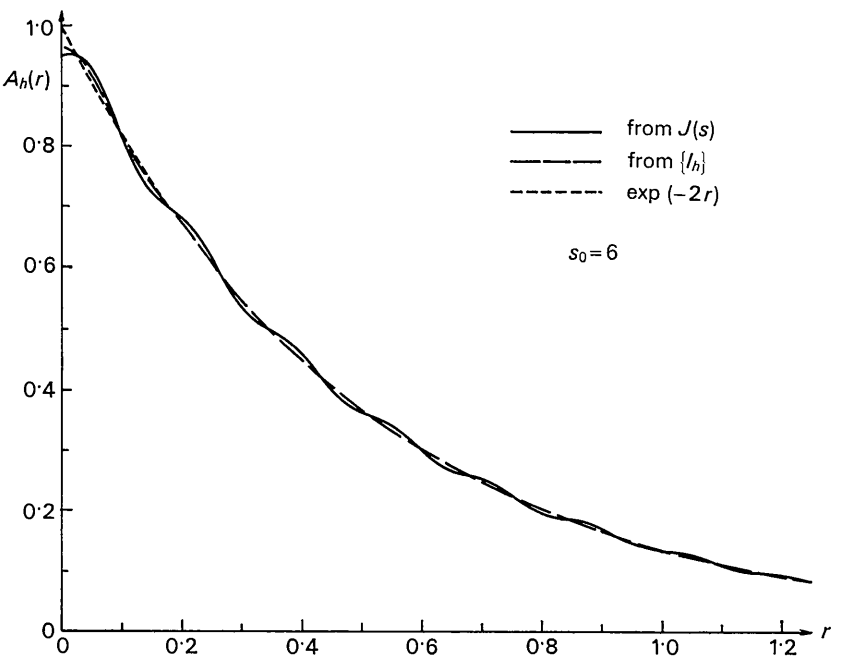

Fig. 9. Line profile analysis of $I(s)$ as given by (36), real part.

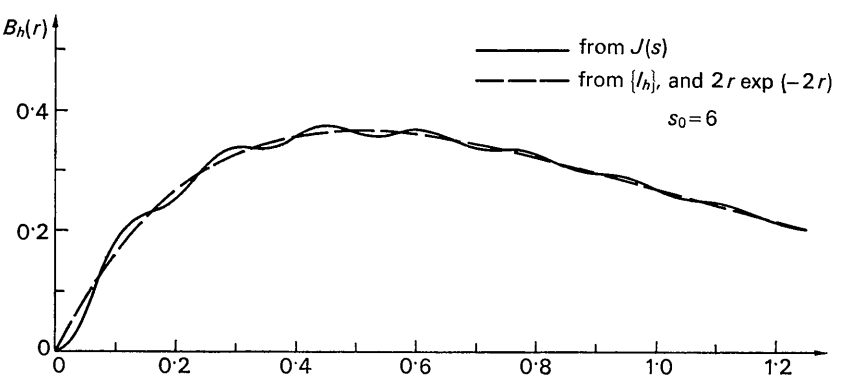

Fig. 10. Line profile analysis of $I(s)$ as given by (36), imaginary part.

$$A_h = \frac{2}{\pi}[\arccos r - r\sqrt{(1-r^2)}]$$

$$B_h = 0 . \quad (35)$$

$$J(s) = \sqrt{\frac{\pi}{2}} F(\pi s) \left[1 - \frac{1}{2\sqrt{(1+\pi^2 s^2)}} + \frac{\pi s}{1+\pi^2 s^2}\right] \quad (36)$$

corresponding to

$$\{I_h\} = \left(\frac{1+\pi s}{1+\pi^2 s^2}\right)^2 ,$$

$$A_h = \exp(-2|r|)$$

$$B_h = 2r \exp(-2|r|)$$

[for $F(z)$ see equation (19)].

Values of A_h and B_h were calculated from $J(s)$, using equations (32) and (33) for various upper limits s_0 (the lower limits were taken as $-s_0$ for simplicity) and compared with A_h and B_h calculated from $\{I\}_h$ with the same truncation, and with the theoretical values. It was found that the optimum value of s_0 depends on the rate at which $J(s)$ is approaching $1/\sqrt{s}$, as could be expected. For the first two test functions (Figs. 7 and 8), calculations with $s_0 = 3$ give already a reasonably good agreement, which means that for such types of distribution a truncation at $s_0 \simeq 1{\cdot}5 b_s$ is admissible. For the last test function (Figs. 9 and 10) a somewhat higher limit ($s_0 = 6$) had to be used, but since this function is rather unlikely to occur in practice [it has been chosen only to demonstrate the applicability of equation (33)] this can be regarded as a limiting case. One can thus expect that, in most of the cases, s_0 values between $1{\cdot}5 b_s$ and $3 b_s$ will be admissible.

The author is indebted to Dr H. Tompa for stimulating discussions during the course of this work, and to Mr J. P. Pauwels for technical assistance.

References

BRINDLEY, G. W. & MÉRING, J. (1951). *Acta Cryst.* **4**, 441.
LAUE, M. VON (1932). *Z. Kristallogr.* **82**, 127.
WARREN, B. E. (1941). *Phys. Rev.* **59**, 693.
WARREN, B. E. & BODENSTEIN, P. (1966). *Acta Cryst.* **20**, 602.
WILSON, A. J. C. (1949). *Acta Cryst.* **2**, 245.

Acta Cryst. (1967). **22**, 623

The Rigid-Body Vibrations of Molecules in Crystals

BY DESMOND M. BURNS, WILLIAM G. FERRIER AND JOHN T. MCMULLAN
Physics Department, University of St. Andrews, Queen's College, Dundee, Scotland

(*Received* 11 *July* 1966)

The rigid-body analysis of the thermal vibrations in seventeen molecular structures has been performed. Parameters are proposed for judging the validity of the rigid-body model by means of an atom-by-atom comparison. It is concluded that the model has a wider range of applicability than might be expected.

Introduction

Since Cruickshank (1956*a*) first introduced the idea, it has become fairly common practice at the end of a molecular crystal structure determination to analyse the anisotropic temperature parameters on the assumption that the molecule is rigid. Often the purpose is no more than the correction of bond lengths (Cruickshank, 1956*b*), and only occasionally has the assumption of rigidity been critically examined. As part of a larger programme of work, it was decided in this laboratory to undertake a survey of suitable molecular structures in order to determine, if possible, the range of validity of the rigid-body approximation. Chosen for analysis were published structures that had been refined to an R index of 0·1 or better, and that not only stated unambiguously the form of their temperature factors but also quoted estimated errors for all temperature parameters. It is surprising, but regrettably true, that published structures can be found from which it is impossible to determine unequivocally what particular form of temperature factor has been used. No structure containing atoms heavier than oxygen was considered, since it was felt that wide disparities in atomic masses might prejudice the validity of the approximation.

Procedure

A program (JMTFAC) was written for the IBM 1620 computer to perform the rigid-body analysis. All published temperature factors were first written in the standard form

$$\exp[-(b_{11}h^2 + b_{22}k^2 + b_{33}l^2 + b_{23}kl + b_{31}lh + b_{12}hk)] ,$$

and were then transformed to U_{ij} referred to orthogonal crystal axes defined by the unit vectors $\hat{\mathbf{b}} \times \hat{\mathbf{c}}^*$, $\hat{\mathbf{b}}$, $\hat{\mathbf{c}}^*$. The transformation equations are: